

Supporting Information

Receptor-Mediated Cellular Uptake Mechanism that Couples to Intracellular Storage

Riki Kawaguchi^{1,2}, Jiamei Yu^{1,2}, Mariam Ter-Stepanian^{1,3}, Ming Zhong¹, Guo Cheng^{1,4}, Quan Yuan², Minghao Jin^{2#}, Gabriel H. Travis^{2,5,6}, David Ong⁷, Hui Sun^{1,2,3,6*}

¹ Department of Physiology, ² Jules Stein Eye Institute, ³ Howard Hughes Medical Institute, ⁴ UCLA-CSST Program, ⁵ Department of Biological Chemistry, David Geffen School of Medicine, University of California, Los Angeles, ⁶ Brain Research Institute, University of California, Los Angeles, ⁷ Department of Biochemistry, Vanderbilt University, [#] Present address: Neuroscience Center, LSU Health Sciences Center

This Supporting Information file contains the following:

- 1. Supplemental Discussion**
- 2. Supplemental Methods**
- 3. Supplemental Figures**
- 4. Supplemental Table**
- 5. Supplemental References**

Supplemental Discussion:

The opposite effects of retinol on STRA6's activity depending on experimental design: The opposite effects of unlabeled free retinol on the retinol fluorescence assay (Figures 3D and 7D) and the ^3H -retinol uptake assay (Figure 7A) are discussed in more detail here. The opposite effects are exactly what are predicted from the final model. The schematic diagrams for these assays are depicted in the second and third diagrams of Figure 8A upper panel. Unlabeled retinol inhibits STRA6-catalyzed retinol release from retinol/RBP but enhances STRA6-mediated ^3H -retinol uptake from ^3H -retinol/RBP because these two assays trace different retinol populations. The radioactive assay specifically traces retinol originally bound to RBP (using ^3H -retinol), while the fluorescence assay traces all retinol bound to RBP. As shown in Figure 8A, when the retinol in RBP is differently labeled from the added free retinol (red vs. black), free retinol would enhance the release of labeled retinol because the unlabeled free retinol competes with the labeled retinol in the loading reaction. By inhibiting the loading reaction of the labeled retinol, unlabeled retinol (in black) enhances the release of labeled retinol (in red). When retinol in RBP is not differentially labeled from the added free retinol, unlabeled free retinol would suppress the release of retinol because the presence of free retinol enhances the loading reaction, which effectively inhibits retinol release. These experiments are two of the key experiments supporting the final model.

Specificity of β -ionone's stimulatory effect on STRA6-mediated vitamin A uptake: The stimulatory effect of β -ionone on vitamin A uptake is highly specific and depends on STRA6. First, in the ^3H -retinol uptake assay from ^3H -retinol/RBP using live cells (Figure 7A), β -ionone has little effect on retinol uptake of control cells but dramatically enhances vitamin A uptake of STRA6 cells. Second, in the retinol fluorescence assays (Figure 7B), β -ionone has no effect on holo-RBP's retinol release when incubated with control membranes but enhances retinol release when STRA6 is present. Third, β -ionone has no effect on STRA6 catalyzed retinol release during the initial phase (indicated by the arrowhead in Figure 7B). This result suggests that β -ionone only starts to show its stimulatory effect when there is a significant amount of retinol released by STRA6, consistent with the role of β -ionone in blocking retinol loading as a means to accelerate retinol release. Indeed, when β -ionone is added during STRA6-catalyzed retinol release, β -ionone's stimulatory effect is much faster (Figure 7C). These real-time measurements demonstrate a further degree of specificity. Fourth, in the vitamin A uptake assay using normal human serum as the source of holo-RBP (Figure 7F), again β -ionone dramatically stimulates cellular vitamin A uptake only when STRA6 is present and has little effect on control cells. These diverse experiments support the high specificity of β -ionone's stimulatory effect on STRA6-mediated vitamin A uptake. The stimulatory effects of β -ionone suggest that LRAT and CRBP-I are not absolutely required for enhanced STRA6 activity and provide further support for the existence of an inhibitory free retinol intermediate as an integral part of the STRA6-mediated retinol uptake process.

LRAT's stimulatory effect on STRA6-mediated vitamin A uptake: Prior to this study, LRAT was the first protein that had been found to stimulate STRA6's vitamin A uptake activity from holo-RBP (1-3). Is LRAT a general stimulator of STRA6's activity (and does STRA6 depend on LRAT like G-protein coupled receptors depend on G proteins)? Previous findings that LRAT does stimulate STRA6's uptake of retinylamine from the retinylamine/RBP complex (3) or the uptake of retinoic acid from the retinoic acid/RBP complex (2) suggest that LRAT is not a general stimulator of STRA6 activity, although it can stimulate STRA6's vitamin A uptake (1-3).

LRAT is a transmembrane domain protein located in intracellular smooth ER (4) and cannot physically interact with STRA6 on the cell-surface membrane. The ability of LRAT to couple to STRA6 independently of CRBP-I strongly suggests that physical interaction with STRA6 is not required for a protein to couple to STRA6. In addition, the following pieces of evidence all suggest that the ability to inhibit the inhibitory free substrate intermediate during STRA6-mediated uptake, not specific physical interaction, is the key mechanism for enhanced STRA6 uptake activity: (1) the ability of CRBP-I to couple to STRA6 for retinol uptake independently of LRAT, (2) the inability of LRAT and CRBP-I to couple to STRA6 for retinoic acid uptake, (3) the ability of CRBP-I to couple to STRA6 for retinoic acid uptake, and (4) the ability of β -ionone to stimulate STRA6-mediated retinol uptake independently of LRAT or CRBP-I.

As shown by diverse experimental evidence, LRAT, CRBP-I and β -ionone enhance STRA6's vitamin A uptake not by enhancing STRA6's retinol release activity, but by inhibiting STRA6's retinol loading activity. It was found previously that a fraction of retinol is loaded back to apo-RBP even in the presence of LRAT (2). If LRAT enhances STRA6's vitamin A uptake because of its ability to inhibit its retinol loading activity, why did retinol loading onto apo-RBP still happen in the presence of LRAT? In our experiments (Figures 4A, 4F and Supplemental Figure 4), LRAT strongly inhibits STRA6-catalyzed vitamin A loading. A hypothesis to explain retinol loss instead of uptake in the presence of LRAT (2) is that retinyl ester hydrolase (5) present in certain cell types can counteract LRAT's activity and make it possible for partial retinol loss to occur.

The human blood maintains micromolar concentrations of holo-RBP under physiological conditions (6). If STRA6 takes up vitamin A from RBP in an uncontrolled manner, cells would be "bloated" with vitamin A. Although both CRBP-I and LRAT can store vitamin A intracellularly and can restrain the random diffusion of retinol, their vitamin A storage mechanisms are different. CRBP-I can be saturated as a retinol binding protein (7). In contrast, LRAT is an enzyme converting retinol to retinyl esters. We found that STRA6/LRAT can take up most if not all retinol bound to RBP in the medium if given sufficient time. For example, STRA6/LRAT depleted most extracellular retinol bound to RBP in 6 hours (grey bars in Supplemental Figure 3). Retinyl ester is a storage form and perhaps the least toxic form of vitamin A that does not diffuse randomly. Indeed, the liver and eye are known to store large quantities of vitamin A in the form of retinyl esters. A cell that specializes in vitamin A storage

(e.g., retinal pigment epithelium cell in the eye) would be overloaded with retinoid in months, if not days, if retinyl esters accumulated in an uncontrolled manner. Although the retinal pigment epithelium cell does take up a large quantity of vitamin A for vision, its retinol uptake and retinol efflux activity need to be controlled and balanced to prevent overloading (8). The identities of proteins involved in regulating retinoid uptake and retinoid efflux are still unknown. Identifying these proteins and elucidating their regulatory mechanisms are interesting topics for future study.

Energy consumption of RBP/STRA6-mediated vitamin A delivery: Unlike primary or secondary active transport, STRA6 does not consume cellular energy during the vitamin A uptake process. Metabolic inhibitors that shut down an energy-dependent process such as endocytosis have no inhibitory effect on STRA6-mediated vitamin A uptake (1). STRA6-mediated vitamin A uptake also happens in a cell-free system without any energy source (1). In addition to its energy independence, STRA6 also does not strictly depend on any intracellular protein for its substrate uptake. STRA6 couples to CRBP-I for retinol uptake, couples to LRAT for retinol uptake, couples to CRABP-I for retinoic acid uptake, and enables β -ionone (which is not an energy source) to greatly enhance cellular vitamin A uptake from holo-RBP. However, because one RBP can only bind to one vitamin A molecule, and RBP eventually gets disposed of in the kidney as apo-RBP due to apo-RBP's inability to bind TTR, the overall energy consumption of the RBP/STRA6 system for specific vitamin A delivery in the blood is much higher than random diffusion by free retinoid, if the synthesis of RBP is taken into account.

Supplemental Methods

Production and purification of holo-RBP, apo-RBP, ^3H -retinol/RBP and ^3H -retinoic acid RBP: Holo-RBP, apo-RBP, and ^3H -retinol/RBP were produced as previously described (1). The high quality of holo-RBP is essential for all experiments. To remove imperfectly folded RBP, it is necessary to use HPLC in order to purify holo-RBP 100% loaded with retinol(1). Poorly folded holo-RBP has low affinity for retinol and can release retinol easily. For production of ^3H -retinoic acid/RBP, ^3H -retinoic acid (PerkinElmer) was incubated with apo-RBP (with 6XHis tag at the N-terminus) overnight at 4°C. ^3H -retinoic acid/RBP was incubated with TALON resin (Clontech) for 3 hours. After 3 washes with PBS, the complex was eluted by 100 mM imidazole in PBS. The eluted ^3H -retinoic acid/RBP was used immediately for the cellular uptake assay.

Assays for ^3H -retinol uptake from ^3H -retinol/RBP and ^3H -retinoic acid uptake from ^3H -retinoic acid/RBP: The human cDNA for CRABP-I was cloned into the mammalian expression vector pRK5. For cellular ^3H -retinol and ^3H -retinoic acid uptake from ^3H -retinol/RBP and ^3H -retinoic acid/RBP, untransfected COS-1 cells or COS-1 cells 24-36 hours after transfection were washed with Hank's Balanced Salt Solution (HBSS) before incubation with ^3H -retinol/RBP or ^3H -retinoic acid/RBP diluted in serum free medium (SFM) for various lengths of time at 37°C. The reactions were stopped by removing the medium, washing the cells with HBSS, and solubilizing the cells in 1% (w/v) Triton X-100 in PBS. Radioactivity was measured with a scintillation counter.

Assay to distinguish between ³H-retinol bound to cell surface in the form of holo-RBP and ³H-retinol transported into the cell during ³H-retinol/RBP as the source of holo-RBP: We used competition by excess unlabeled holo-RBP after ³H-retinol uptake assay from ³H-retinol/RBP as a way to detect ³H-retinol/RBP bound to the cell surface. Briefly, the cells were washed with HBSS and incubated with ³H-retinol/RBP diluted in SFM for 1 hour; then the medium containing ³H-retinol/RBP was removed and the cells were again washed with HBSS. Excess unlabeled holo-RBP (6-8 µg/ml) diluted in SFM was added to the cells for a 1 hour incubation. Radioactivity in the medium and radioactivity remaining in the cells were separately counted.

Assay to distinguish between retinol bound to cell surface in the form of holo-RBP and retinol transported into the cell using human serum as the source of holo-RBP: In nonradioactive vitamin A uptake assays, we removed RBP bound to STRA6 on the cell surface by taking advantage of the transient nature of the RBP/STRA6 interaction. For retinol uptake assay using human serum as the source of holo-RBP, we first incubated transfected or untransfected COS-1 cells with 25% (v/v) normal human serum diluted in SFM (Innovative Research) for six hours. After the incubation, cells were washed once with HBSS. To remove RBP bound to the cell surface, cells were further incubated in SFM for two hours. At the one-hour interval, the cells were washed once more with SFM. We have shown that there was no detectable RBP associated with cell surface after the two-hour incubation in SFM (Figure 1F).

Purification of the RBP/TTR complex from human serum: Five milliliters of normal human serum (Innovative Research) were exhaustively dialyzed against 400 ml of 0.1M sodium acetate, pH 5.6, with constant stirring at 4°C overnight. After dialysis, the sample was spun at 14,000 g for 3 min at 4°C to removed precipitants. The dialyzed serum was gently applied to a DEAE Sephadex A-50 column (20 ml bed volume) pre-equilibrated with 0.1M sodium acetate, pH 5.6. After all serum entered the column, 2 ml 0.1M sodium acetate, pH 5.6 was added to the column before the column was washed by 20 ml of 0.3M sodium acetate buffer, pH 5.6, and 10 ml of 0.3 M sodium acetate buffer, pH 5.4. The elution was carried out using 20 ml 1M sodium acetate, pH 5.1. One milliliter fractions were collected. Fractions containing RBP were monitored using retinol fluorescence. Five to ten peak fractions containing holo-RBP (about 5 ml) collected from the DEAE Sephadex column were dialyzed against 400 ml of PBS overnight at 4°C with constant stirring. The dialyzed sample was gently applied to the Q-Sepharose column (10 ml bed volume) pre-equilibrated with PBS. After the sample entered the column, the column was first washed with 10 ml of 0.2 M sodium chloride and 10 ml of 0.3 M sodium chloride in PBS, and then eluted with 10 ml of 0.4 M sodium chloride in PBS and 10 ml of 0.5 M sodium chloride in PBS. Fractions containing RBP were monitored using retinol fluorescence. The peak fractions containing RBP are usually the fractions during the transition between 0.3 M NaCl and 0.4 M NaCl elutions. For HPLC purification of RBP/TTR complex, the peak fractions containing RBP from Q-Sepharose were dialyzed against 25 mM Tris, pH 8.0 with 120mM NaCl overnight. Samples were then concentrated and injected into HPLC using weak anion exchange column AX-300 (Eprogen). Proteins are separated with NaCl step gradient (120 mM for 5 min, 220 mM

for 10 min and 2 M for 15 min) at 1ml/min. Peak retention times for RBP and RBP/TTR are usually 9.3 min and 13.2 min, respectively.

Production and purification of apo-CRBP-I, EGFP-CRBP-I, and EGFP-CRBP-II: Apo-CRBP-I, EGFP-CRBP-I and EGFP-CRBP-II were produced in mammalian cells by transfection of 6XHis tagged versions of the proteins and nickel affinity purification (EGFP is connected to CRBP-I and CRBP-II through a 3 glycine linker). Briefly, 48 hours after transfection using JetPrime transfection reagent (Polyplus Transfection), COS-1 cells were harvested and lysed in 1% Triton-X-100 in PBS with protease inhibitors by grinding. After pelleting down insoluble materials and cell nuclei at 16,000 g at 4°C for 30 min, the soluble materials were incubated with Ni-NTA resin (Qiagen) for 5 hours at 4°C. After 2 washes in 1% Triton X-100 in PBS, 3 washes in PBS containing 1M NaCl, and 2 washes in PBS, the tagged protein was eluted in 150 mM imidazole in PBS.

HPLC analysis of cellular retinol or retinyl ester content after uptake from holo-RBP or human serum: Retinyl ester was extracted by adding methanol containing 1mM 2,6-Di-tert-butyl-4-methylphenol to the cell pellet and vigorously mixing for 5 min. Cell debris were pelleted at 5,000g for 5 min at 4°C. Extraction of retinyl ester was repeated 3 times, and the extracts were pooled. Samples were analyzed on an Agilent 1100 series liquid chromatography system with a photo-diode array detector. Retinyl ester was separated by reverse phase chromatography using a ZORBAX Eclipse EDB-C18 column (Agilent). The isopropanol concentration was increased from 0 to 100% against methanol during the 10 min run, followed by a 5 min wash with 100% isopropanol. Retinyl ester levels were normalized using methanol soluble proteins and peptides, which come out at 2.4 min (absorbance at 280 nm). Retinol from cells was extracted using hexane containing 1 mM BHT. Retinol was dried under nitrogen and then resolubilized in 100% methanol. Before HPLC analysis, water was added to the solution so that the methanol concentration was 90%. Retinol was separated using a ZORBAX Rx-SIL column (Agilent) and using 90% methanol as the mobile phase. Both retinyl esters and retinol were detected by absorbance at 325 nm. A peak representing hexane soluble peptides was used as an internal loading control.

Monitoring retinol fluorescence using a fluorometer: We developed an assay to study retinol release from holo-RBP based on its dramatically enhanced fluorescence when bound to RBP (9). Membranes prepared from transfected or untransfected COS-1 cells were washed twice with PBS, resuspended in PBS, passaged through gastight 22s gauge syringe (Hamilton) six times before being used in fluorescence assays. The full emission spectra were measured using Fluorolog FL3-21 (Jobin Yvon) with excitation at 330 nm for retinol. The emission spectrum of each reaction was obtained from 360 to 600 nm with 1 nm increment and 5 nm slit width. Data was analyzed DataMax (Instruments SA, Inc.) and Grams/32 software (Galactic Industries Corp).

Simultaneous real-time monitoring of the retinol fluorescence for multiple reactions: Real time monitoring of retinol fluorescence was measured using a fluorescent microplate reader

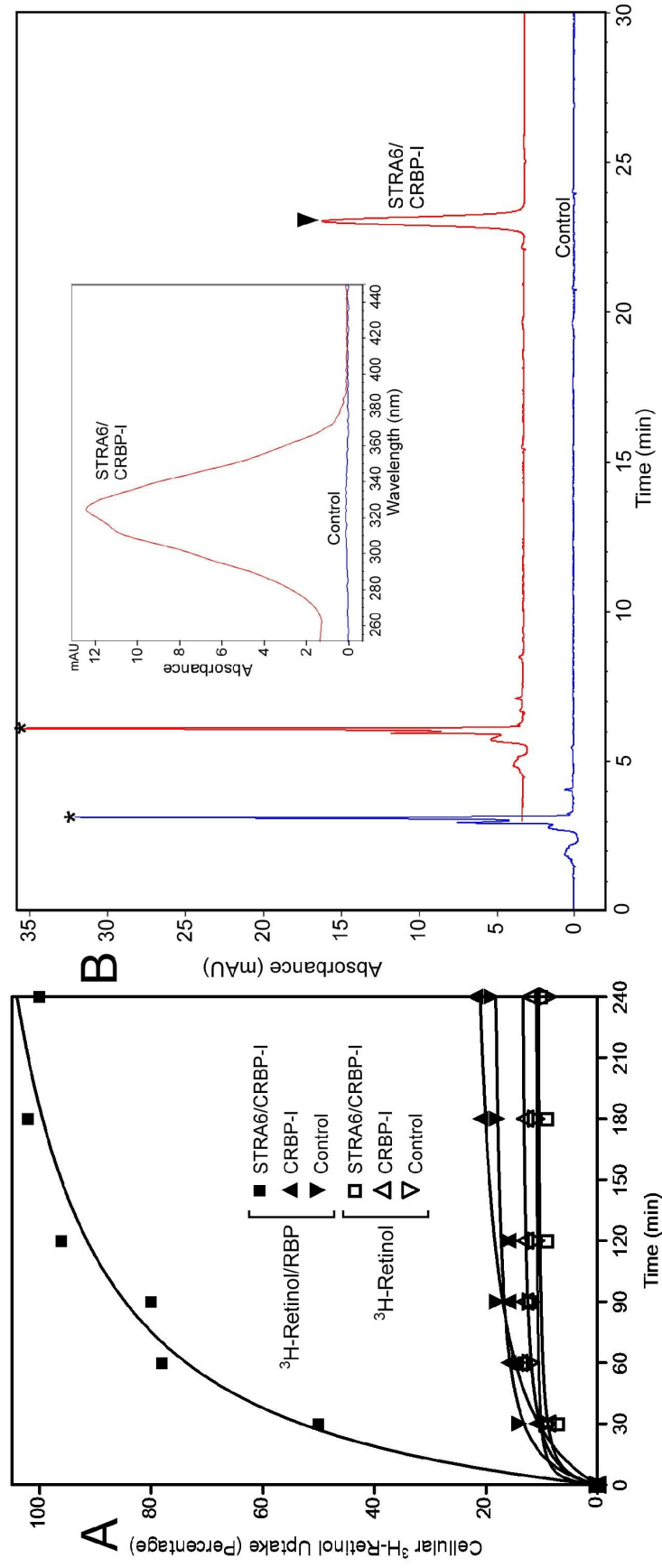
POLARstar Omega (BMG LABTECH) with the excitation filter 320ex and the emission filter 460-10. The signal from each time points is the average of 10 measurements. Samples were shaken for 10 sec at 500 rpm using double-orbital shaking before each measurement. Membranes resuspended in PBS and mixed with various proteins were transferred to a black Microfluor-2 plate (Thermo) for fluorescent measurement. The Microfluor-2 plate was precoated with Blocker Casein (Pierce) overnight at 4°C and washed once with PBS before addition of membrane suspension to prevent nonspecific sticking of holo-RBP to the plastic wall. For all fluorescence measurements, the fluorescent signals before the addition of retinol or holo-RBP at 0 min are considered background signals and were subtracted from the final fluorescence signals at different time points. Although the background signals are low compared to retinol fluorescence in holo-RBP, subtracting the background eliminates the nonspecific influence of light scattering from the membranes and makes it possible to focus on the retinol fluorescence of holo-RBP or retinol added at 0 min. In the assay to study the effect of retinol dehydrogenase (RDH) and NAPD STRA6-catalyzed retinol release, photoreceptor RDH (*10*) was cotransfected with STRA6.

Fluorescence resonance energy transfer (FRET) between retinol and EGFP: FRET can be employed to monitor dynamic molecular interactions (*11*). We designed a new FRET pair using retinol as the donor and EGFP (*12*) as the acceptor by taking advantage of the fact that the emission spectrum of retinol overlaps significantly with the excitation spectrum of EGFP (Supplemental Figure 4A). Since CRBP-I forms a complex with retinol, retinol-EGFP FRET should be observed when retinol is bound to EGFP-CRBP-I fusion protein given the close distance between retinol and EGFP. Strong steady-state FRET between retinol and EGFP when retinol is bound to EGFP-CRBP-I was demonstrated by observing the dequenching of retinol (donor) fluorescence after quenching EGFP (acceptor) fluorescence (Supplemental Figure 4B). EGFP bleaching was done using the XLamp XR-E Blue LED (465-485 nm) (CREE) with the samples in the well of a white 96-well plate (Falcon). Full emission spectra were measured using Fluorolog FL3-21 (Jobin Yvon). For each time point, samples were scanned twice and signals were averaged. To specifically track the fate of retinol of the holo-RBP or retinol added at 0 min, we subtracted the background signal of each reaction before the addition of holo-RBP or retinol.

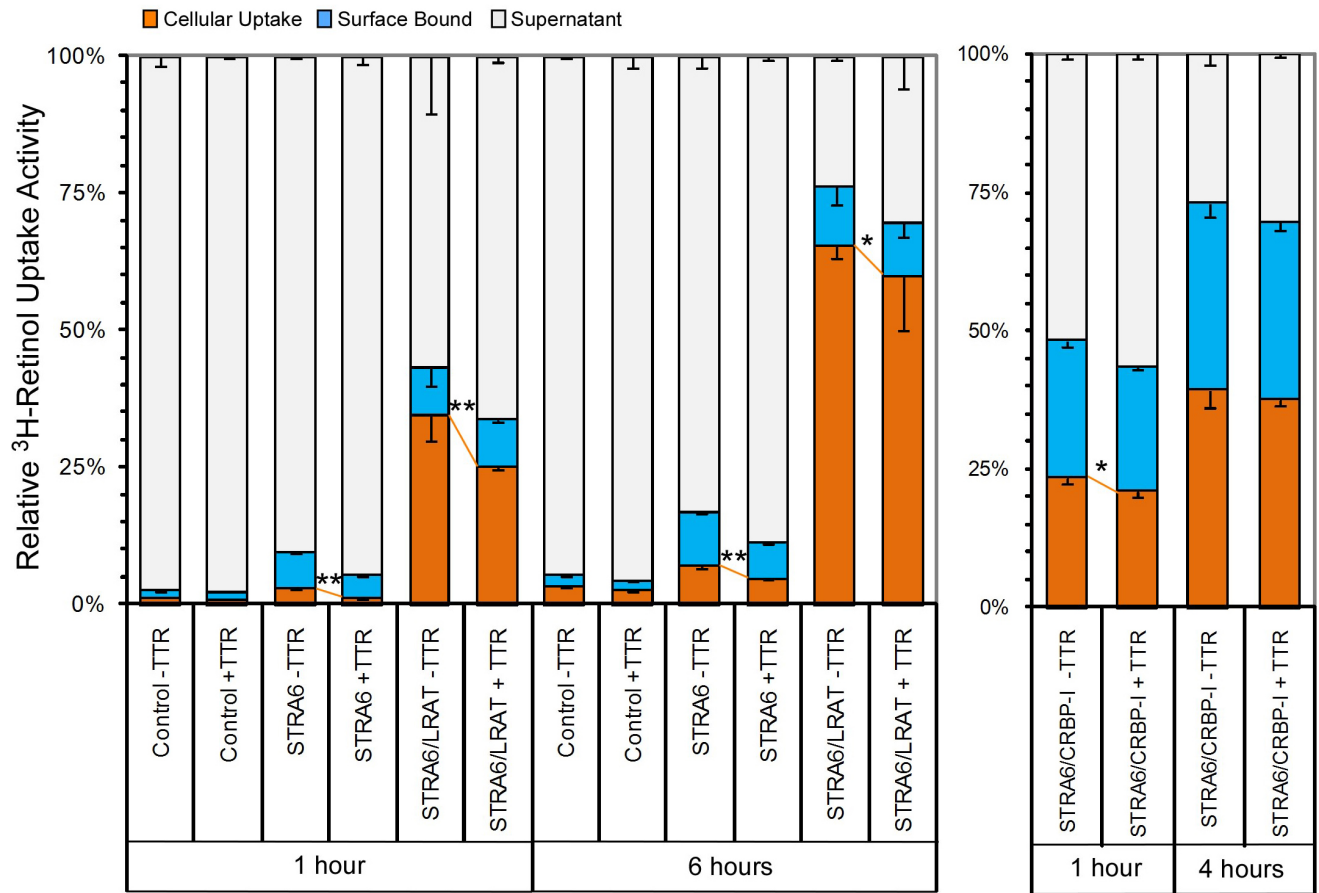
Simultaneous real-time measurement of FRET between retinol and EGFP for multiple reactions: For real-time simultaneous FRET measurement of multiple reactions, we measured the dynamic change in the ratio of the acceptor/donor emission peaks (*13*). The feasibility of this approach was first demonstrated by the concomitant increase in the EGFP fluorescence emission peak and the decrease in the retinol fluorescence emission peak during the STRA6-catalyzed transport of retinol from holo-RBP to EGFP-CRBP-I (Figure 5A). Real-time retinol-EGFP FRET was measured using POLARstar Omega with the excitation filter 320ex and the emission filters 460-10 and 510-10 using simultaneous duel emission optics. The signal from each time point of each reaction was the average of 10 measurements. The fluorescence of each reaction was measured before holo-RBP or retinol is added at 0 min to initiate the reaction. The equation

to calculate this ratio is $[(510_t - 510_b)/(460_t - 460_b)]$, where 510_t , 510_b , 460_t , and 460_b represent emissions at 510 nm after initiation of the reaction (t=time point), at 510 nm before retinol or holo-RBP is added (b=background), at 460 nm after initiation of the reaction (t=time point), and at 460 nm before retinol or holo-RBP is added (b=background), respectively. This method eliminates the contribution of FRET-independent decrease in donor (retinol) fluorescence signal due to retinol release from holo-RBP, as demonstrated by the fact that the STRA6-induced decrease in retinol fluorescence alone does not cause this ratio change (Figure 5C). The specificity is also demonstrated by the time-dependence of the signal, the retinol and EGFP-CRBP-I-dependence of the signal (retinol and EGFP do not generate this signal), and its suppression by apo-CRBP-I.

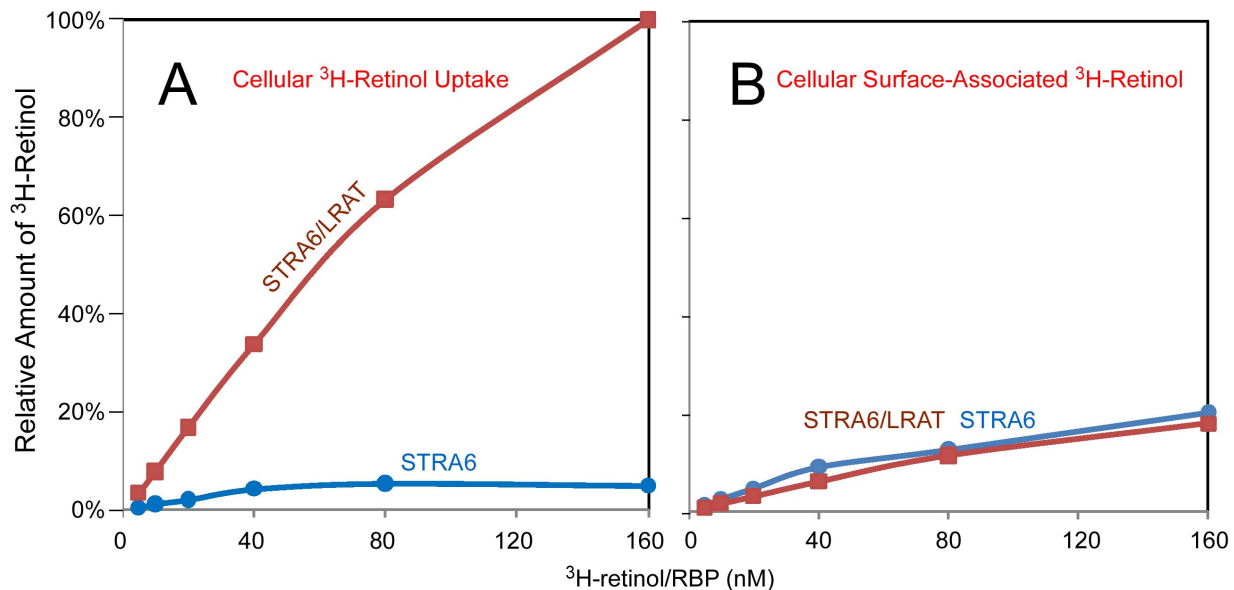
Supplemental Figures



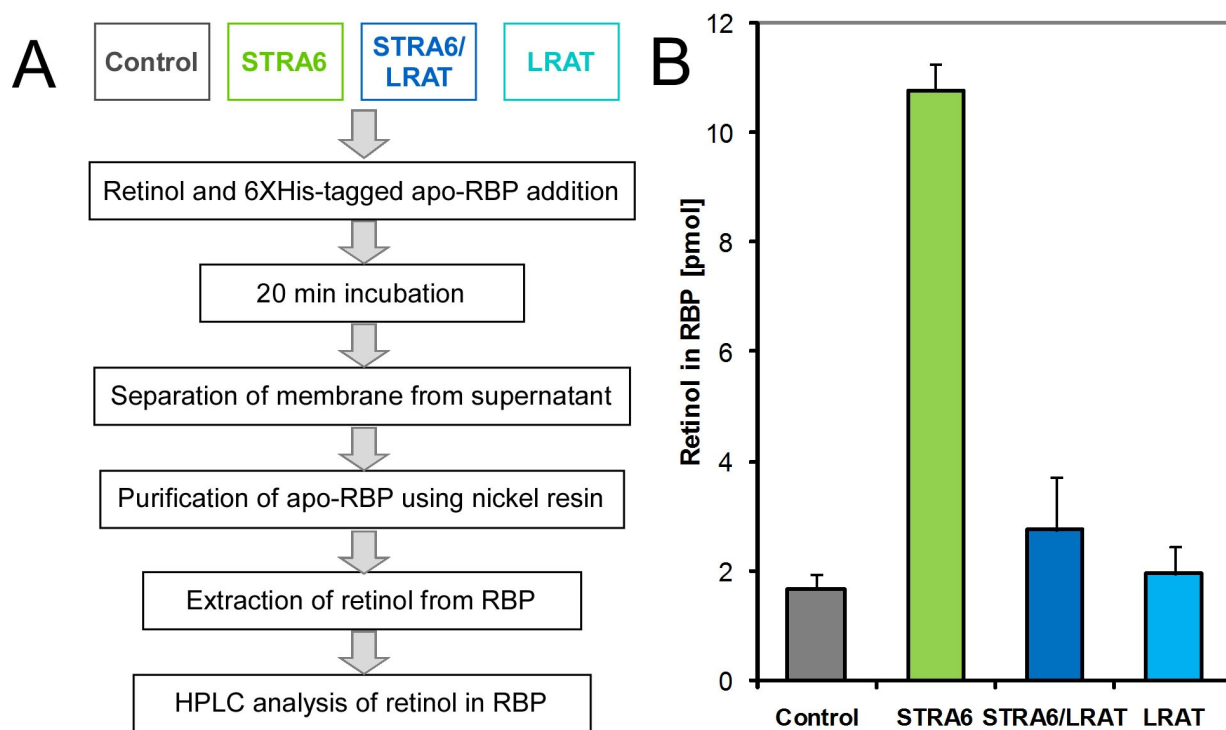
Supplemental Figure 1. STRA6-mediated retinol uptake from holo-RBP is enhanced by CRBP-I. **(A)** Comparison of the time courses of ³H-retinol uptake from ³H-retinol/RBP for STRA6/CRBP-I, CRBP-I and control cells (filled symbols). Also included in the comparison are the time courses of ³H-retinol uptake from free ³H-retinol for STRA6/CRBP-I, CRBP-I and control cells (open symbols). Both 3H-retinol/RBP and free ³H-retinol concentrations are 3.8 nM. The highest 3H-retinol uptake activity of STRA6/CRBP-I cells is defined as 100%. The absence of enhanced uptake of STRA6/CRBP-I cells for free retinol demonstrates that STRA6 is not a transporter for free retinol and does not facilitate retinol uptake unless it is associated with RBP. **(B)** HPLC analysis of cellular uptake of retinol. STRA6/CRBP-I cells and control cells were assayed by HPLC for vitamin A uptake from 25% human serum (4 hours of incubation). Retinol was extracted by hexane and separated by HPLC. HPLC profiles of hexane extracts are shown. Arrowhead indicates the peak for retinol. Asterisks indicate hexane soluble peptides used as internal loading control. Inset, absorption spectrum of the retinol peak for STRA6/CRBP cells (as indicated by an arrowhead in B).



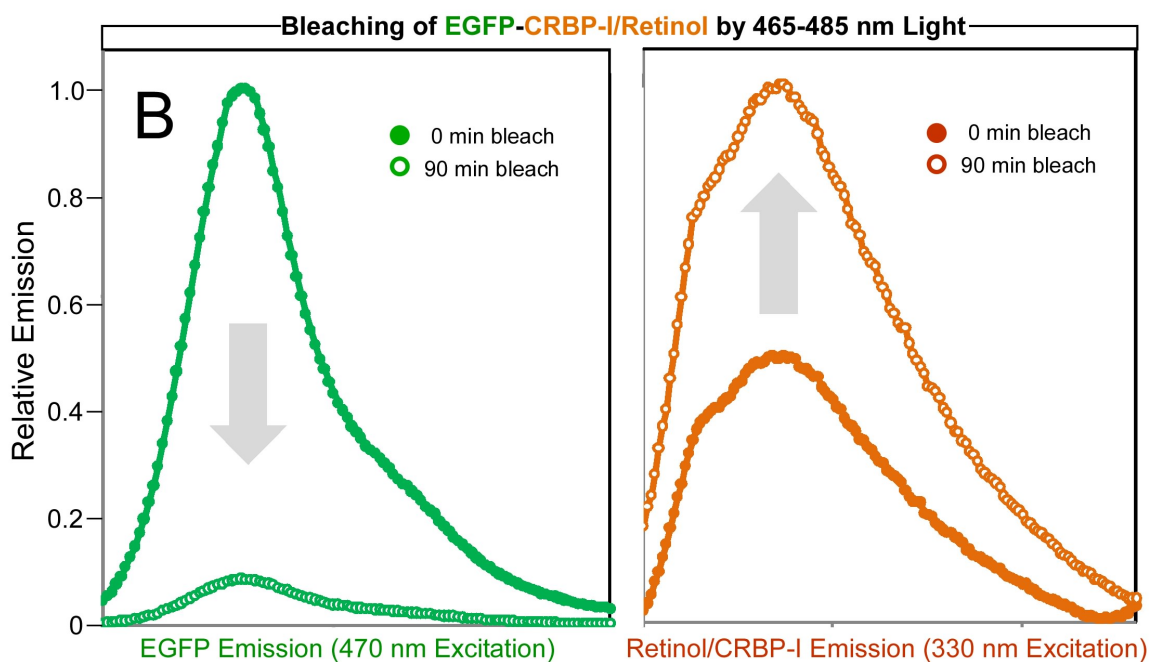
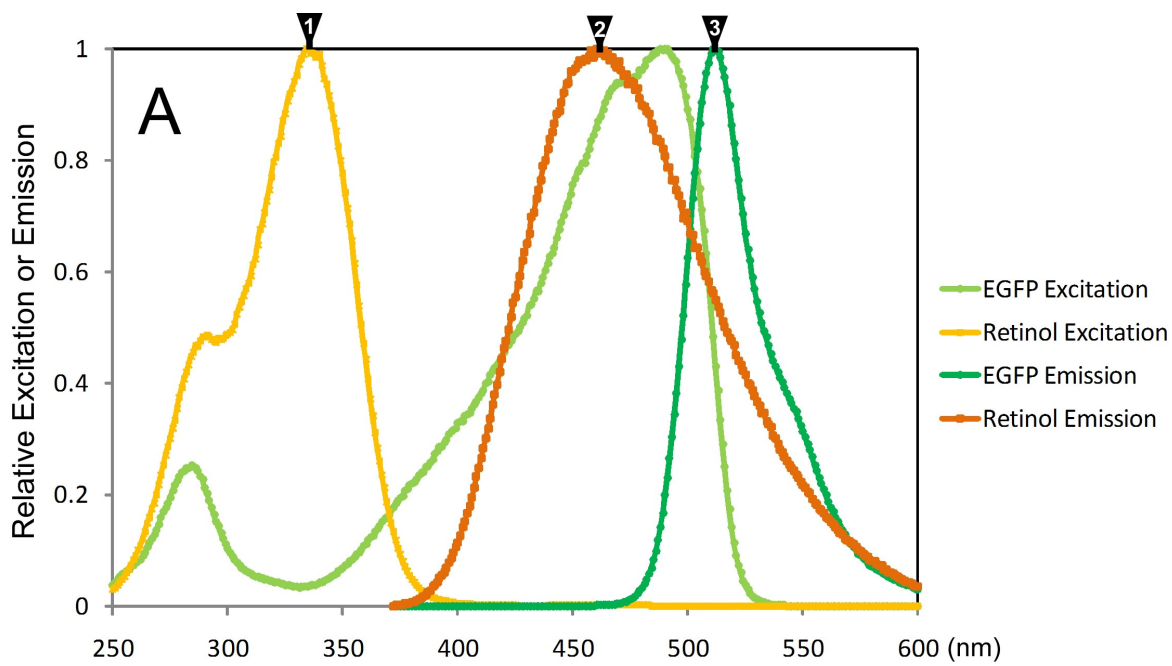
Supplemental Figure 2. TTR partially suppresses STRA6-mediated vitamin A uptake from holo-RBP. STRA6 only, STRA6/LRAT or control cells were incubated with ^3H -retinol/RBP or ^3H -retinol/RBP complexed with TTR for ^3H -retinol uptake. After removing the supernatant, the cells were washed once with serum free medium (the wash was counted as part of the supernatant). Excessive unlabeled holo-RBP in serum free media was added to each well for 1 hour to remove surface bound ^3H -retinol/RBP. The cells were lysed in 1% Triton X-100 in PBS. Radioactivity associated with the supernatant, the cell surface (removed by excessive unlabeled holo-RBP), and the cells were counted and shown as a percentage of the total radioactivity added to the cells. This experiment showed that TTR partially, but not completely, suppresses STRA6-mediated vitamin A uptake from holo-RBP. Significant suppression by TTR is indicated by asterisks (*: $p < 0.05$, **: $p < 0.01$). P values were determined by two-tail Student t-test. Because of the low retinol uptake activity of STRA6-only cells, TTR has a bigger impact on these cells than on STRA6/LRAT cells and STRA6/CRBP-I cells. For example, at one hour, the cellular uptake activity of STRA6/LRAT cells was 12 times the activity of STRA6-only cells without TTR, but 21 times with TTR.



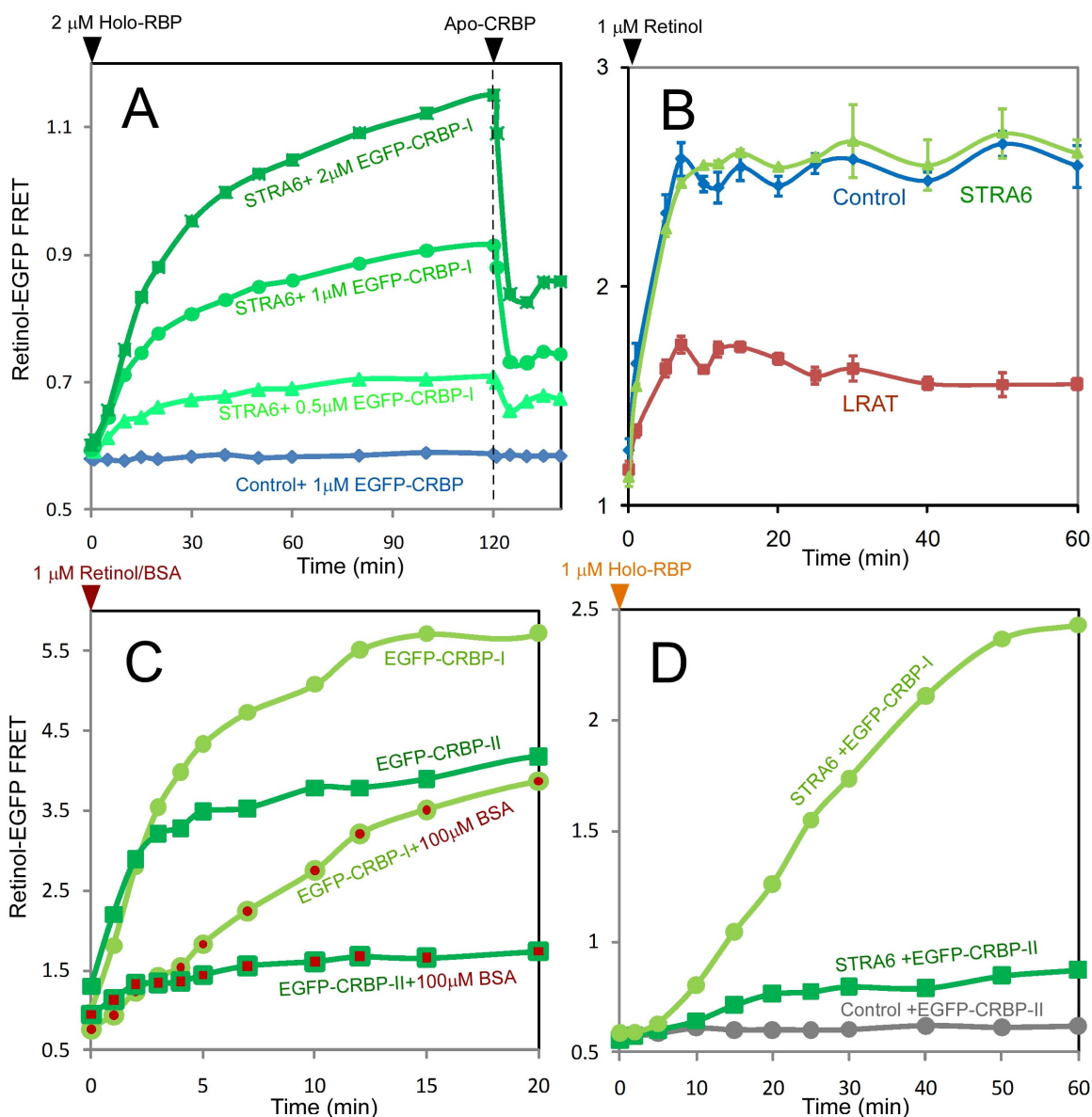
Supplemental Figure 3. LRAT's stimulatory effect on STRA6's vitamin A uptake activity is more pronounced in the ³H-retinol uptake assay when more ³H-retinol/RBP is added. **(A)** Cellular ³H-retinol uptake (³H-retinol in the form of surface bound holo-RBP has been subtracted) in STRA6-only cells reaches a plateau much more quickly than in STRA6/LRAT cells. **(B)** ³H-retinol associated with cell surface bound RBP. No significant difference was observed for surface bound ³H-retinol/RBP between STRA6 only and STRA6/LRAT cells. Cell surface bound ³H-retinol/RBP was removed by incubating cells with excessive unlabeled holo-RBP. For both figures, the highest activity (cellular uptake for STRA6/LRAT) is defined as 100%. Consistent with the retinol fluorescence assay, this experiment showed that LRAT's enhancement effect on STRA6's vitamin A uptake activity is more pronounced when there is more holo-RBP.



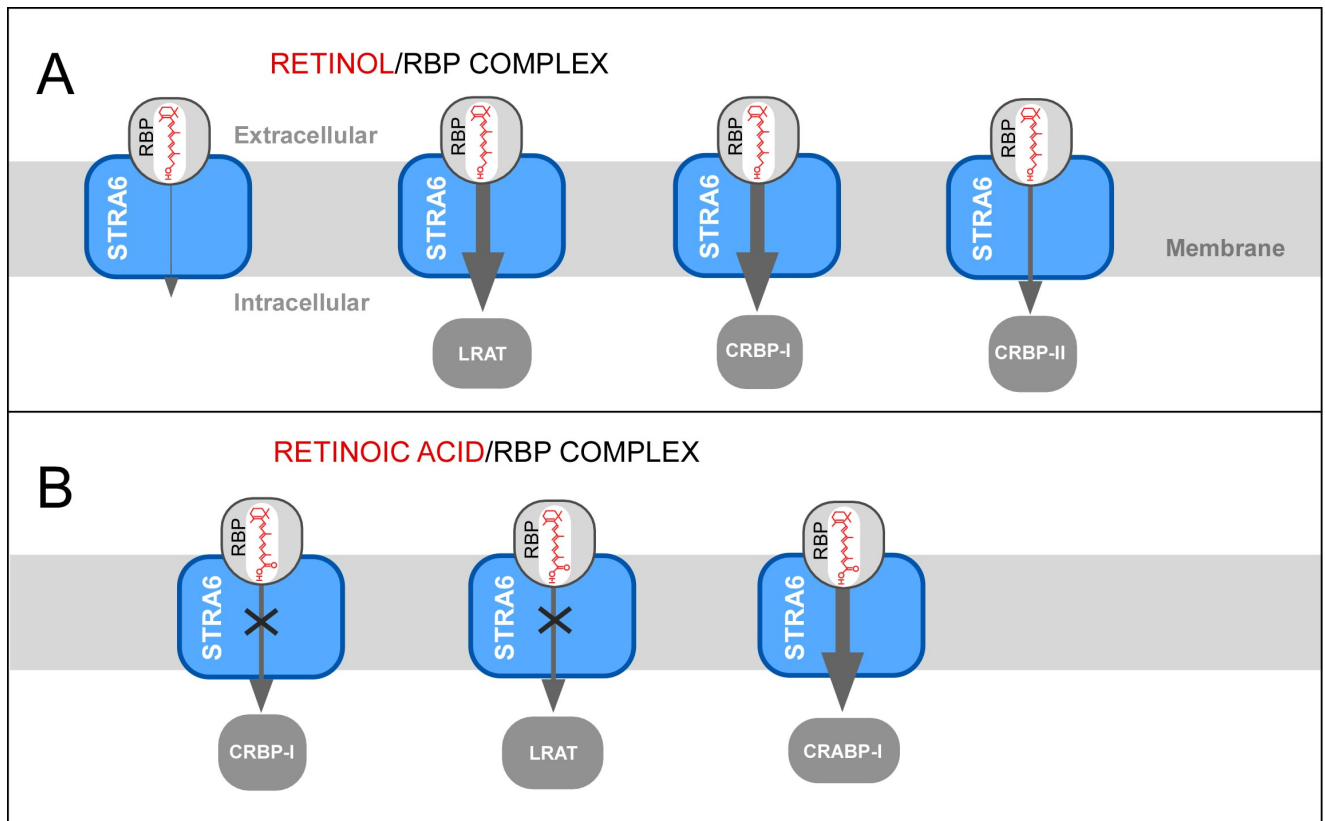
Supplemental Figure 4. HPLC analysis of STRA6-mediated retinol loading into apo-RBP and its inhibition by LRAT. **A.** Diagram of experimental procedure. Retinol (2 μ M) and apo-RBP (2 μ M), which has a 6XHis tag at the N-terminus, were added to control, STRA6, STRA6/LRAT or LRAT membranes (50 μ l reaction volume). After 20 min of incubation, the supernatant was separated from the membrane by centrifugation. RBP was purified from the supernatant of each reaction using nickel resins. Retinol was then extracted from the purified RBP and analyzed by HPLC. **B.** Retinol loaded into RBP was quantified using HPLC analysis of retinol extracted from purified RBP.



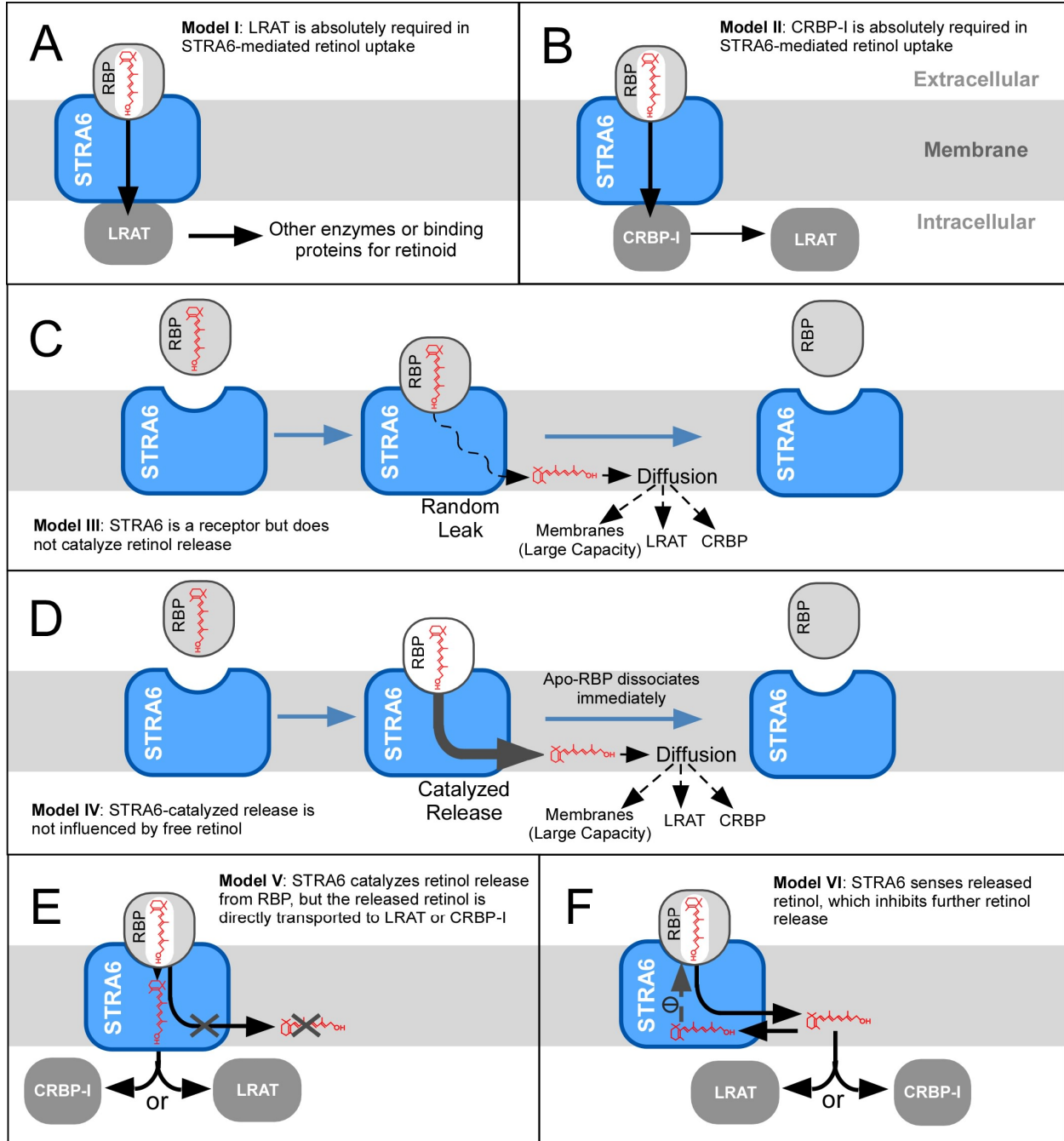
Supplemental Figure 5. Retinol-EGFP FRET. **(A)** Normalized excitation and emission spectra of retinol and EGFP showing significant overlap between the emission spectrum of retinol and the excitation spectrum of EGFP. The peak wavelength for exciting retinol, and the peak emission wavelengths of retinol and EGFP are indicated by arrowheads 1, 2, 3, respectively. **(B)** Bleaching EGFP leads to regaining of retinol fluorescence in EGFP-CRBP-I bound with retinol. EGFP fluorescence was bleached for 90 min using a 465-485 nm LED light source. FRET efficiency of retinol-EGFP FRET for retinol bound to EGFP-CRBP-I is about 48%.



Supplemental Figure 6. Real-time monitoring of retinol binding by EGFP-CRBP-I and EGFP-CRBP-II using retinol-EGFP FRET. **(A)** EGFP-CRBP-I concentration-dependence of the FRET signal. Holo-RBP was added at 0 min to all reactions containing STRA6 membranes or control membranes and different amounts of EGFP-CRBP-I. At 120 min, an equal amount of apo-CRBP-I (as EGFP-CRBP-I) was added to each reaction. Although all reactions started from the same initial signal, retinol-EGFP FRET signal increases in an EGFP-CRBP-I concentration and STRA6 dependent manner. **(B)** CRBP-I absorbs retinol added to control membranes indistinguishably from STRA6 membranes. At 0 min, 1 μM of retinol was added to STRA6, LRAT, or untransfected membrane premixed with 1 μM of EGFP-CRBP-I. A time-dependent increase in FRET signal between retinol and EGFP was observed for reactions containing STRA6 or control membranes, but was suppressed in the reaction containing LRAT. **(C)** Transfer of retinol from 1 μM retinol/BSA complex (added at 0 min) to EGFP-CRBP-I (1 μM) and EGFP-CRBP-II (1 μM). Retinol was rapidly transferred from BSA to both EGFP-CRBP-I and CRBP-II in the absence of additional BSA. However, 100 μM retinol-free BSA, which binds to small molecules including retinol promiscuously, largely suppressed the transfer of retinol to EGFP-CRBP-II and slowed down the transfer to EGFP-CRBP-I. This experiment is consistent with the much lower affinity of CRBP-II for retinol compared with CRBP-I. **(D)** Retinol-EGFP FRET analysis showing that the STRA6-catalyzed transfer of retinol from holo-RBP (1 μM) to EGFP-CRBP-II (0.5 μM) is much less effective than to EGFP-CRBP-I (0.5 μM).



Supplemental Figure 7. Summary schematic diagram showing STRA6's coupling to specific intracellular storage proteins to mediate substrate uptake. **(A)** STRA6 by itself takes up little vitamin A from holo-RBP, but has greatly enhanced vitamin A uptake activity in the presence of either LRAT or CRBP-I. CRBP-II is much less effective than CRBP-I in coupling to STRA6. This difference is a result of the lower affinity of CRBP-II in binding retinol. The fact that both CRBP-II and the membrane bind retinol but cannot effectively couple to STRA6 suggests the ability to bind retinol is not sufficient to couple to STRA6. **(B)** STRA6-mediated retinoic acid uptake from retinoic acid/RBP is coupled to CRABP-I, but not to CRBP-I or LRAT. This further demonstrates the specificity of STRA6's coupling to intracellular retinoid storage proteins.



Supplemental Figure 8. Possible models of STRA6-mediated vitamin A uptake. All models presented here were considered during different stages of this work, but turned out not to be supported by experimental evidence. **(A)** In model I, STRA6 strictly depends on LRAT to take up vitamin A. This model might explain the large stimulatory effect of LRAT on STRA6's vitamin A uptake activity as observed in previous studies. In this model, retinol taken up by LRAT is subsequently delivered to other retinoid processing enzymes or retinoid binding protein like CRBP-I. The ability of CRBP-I to couple to STRA6 for retinol uptake, the ability of CRBP-I to couple to STRA6 for retinoic acid uptake, the inability of LRAT to couple to

STRA6 for retinoic acid uptake, and the ability of β -ionone to stimulate STRA6-mediated vitamin A uptake independent of LRAT all argue against this possibility. In addition, LRAT's intracellular localization to smooth ER (14) makes it unlikely to physically interact with STRA6 located on cell surface. **(B)** In model II, STRA6 strictly depends on CRBP-I to take up vitamin A. Retinol taken up by CRBP-I is subsequently delivered to other retinoid processing enzymes such as LRAT. This model is the most popular and the most frequently proposed model for RBP receptor mechanism. This model is reasonable given the stimulatory effect of CRBP-I on STRA6 activity and the ability of CRBP-I to provide retinol to LRAT. However, the ability of LRAT to couple to STRA6 for retinol uptake independently of CRBP-I, the ability of CRBP-I to couple to STRA6 for retinoic acid uptake, the inability of CRBP-I to couple to STRA6 for retinoic acid uptake, and the ability of β -ionone to stimulate STRA6-mediated vitamin A uptake independent of CRBP-I all argue against this possibility. In addition, apo-CRBP-I takes up free retinol efficiently regardless whether STRA6 is present or not. This property is in sharp contrast to apo-RBP, which depends on STRA6 for efficient retinol loading and suggests that CRBP-I, like LRAT, act on free retinol released from STRA6. **(C)** In model III, STRA6 acts only as a receptor to target RBP to a particular cell, but does not catalyze retinol release. In this model, retinol leaks out of RBP and diffuses into cellular membranes, which have almost unlimited capacity to store the hydrophobic retinol. Leaked retinol is also picked up by LRAT and CRBPs. The clear ability of STRA6 to facilitate retinol release from holo-RBP and the coupling of STRA6-mediated retinol uptake to retinoid storage proteins argue against this model. **(D)** In model IV, STRA6 is a receptor and catalyzes retinol release from RBP, but the released retinol does not affect further retinol release. This model is possible if RBP dissociates from STRA6 immediately after losing retinol, in analogy to RBP's immediate loss of binding to TTR after losing retinol (15). The fact STRA6-mediated retinol uptake is coupled to LRAT and CRBP-I but not to the membrane argues against this model. **(E)** In model V, STRA6 catalyzes retinol release from holo-RBP but retinol is directly transported through STRA6 to LRAT or CRBP-I. Although this model may explain the strict coupling between STRA6 and LRAT or CRBP-I, independent experimental evidence supports the presence of the free retinol intermediate. First, free retinol enhances STRA6-mediated ^3H -retinol uptake from ^3H -retinol/RBP, but free retinol inhibits STRA6-mediated retinol uptake from unlabeled holo-RBP. In contrast, the retinol analog β -ionone enhances both ^3H -retinol uptake from ^3H -retinol/RBP and retinol uptake from unlabeled holo-RBP. The opposite effects of free retinol and the uniform effect of β -ionone cannot be explained without the presence of a free retinol intermediate and the inhibitory retinol loading pathway as an integral part of STRA6-mediated retinol uptake process. The stimulatory activities of both retinol and β -ionone can be explained by blocking the activity of STRA6 to load free retinol. Second, STRA6's efficient loading of free retinol into apo-RBP is a direct demonstration of the loading pathway starting from free retinol. Third, RDH and NADP enhance STRA6-mediated retinol release. Free retinol is the substrate for RDH. Fourth, apo-CRBP-I takes up free retinol equally efficiently regardless whether STRA6 is present or not. Consistently, LRAT can also directly act on free retinol. **(F)** In model VI, STRA6 catalyzes retinol release from RBP, but the released retinol inhibits further retinol release through a negative feedback mechanism. LRAT and CRBP-I couple to STRA6 because they can remove the inhibitory free retinol. The fact that free unlabeled retinol (or its analog β -ionone) enhances, not inhibits, STRA6-mediated ^3H -retinol uptake from ^3H -retinol/RBP argues against this model.

Supplemental Table: Summary of Experimental Evidence and Techniques

| Figures | Experimental Designs | Techniques | Measurements | Time Points Per Condition | Repeats |
|------------------------------|---|--|------------------|--|---------|
| Figure 1B | STRA6's coupling to CRBP-I and CRBP-II in cellular retinol uptake | Cellular ³ H-retinol uptake from ³ H-retinol/RBP complex | 6X3 = 18 | 60 min | 3 |
| Figure 1C | Time courses STRA6-mediated retinol uptake | Cellular ³ H-retinol uptake from ³ H-retinol/RBP complex | 5X3 = 15 | 0, 15, 30, 60, 120, 180 min | 3 |
| Figure 1D | Removal of cell surface bound RBP in retinol uptake assay from holo-RBP | Cellular ³ H-retinol uptake from ³ H-retinol/RBP complex | 4X3 = 12 | 60 min | 6 |
| Figure 1E | Dependence of LRAT on retinyl ester formation during retinol uptake | HPLC analysis for cellular retinol uptake from human serum | 3 | 4 hours | 3 |
| Figure 1F | Time course of RBP binding to cell surface | Analysis of RBP bound to cell surface using Western blot | 6 | 0, 60, 120 min | 4 |
| Figure 1G | Removal of cell surface bound RBP in retinol uptake assay from human serum | HPLC analysis for cellular retinol uptake from human serum | 12 | 4 hours | 3 |
| Figure 2A | STRA6-mediated retinol release from holo-RBP | Retinol fluorescence assay for retinol release from holo-RBP | 5 | 2 hours | 3 |
| Figure 2B | Fractionation of membrane and supernatant in the retinol release assay | Retinol fluorescence assay for retinol release from holo-RBP | 10X3 = 30 | 2 hours | 3 |
| Figure 2C | Retinol in the supernatant is in the form of holo-RBP after retinol release | Retinol fluorescence assay for retinol release from holo-RBP | 6X3 = 18 | 2 hours | 3 |
| Figure 2D | The fate of retinol in the membrane after retinol release from holo-RBP | HPLC analysis of retinol and retinyl esters | 6 | 2 hours | 3 |
| Figure 3A | Multi-step purification of the holo-RBP/TTR complex from human serum | DEAE sepharose, Q sepharose, and Polyethyleneimine columns | 4 | N/A | 5 |
| Figure 3B | STRA6-mediated retinol release from holo-RBP/TTR complex | Real-time monitoring of retinol release from RBP/TTR complex | 4X15X10 = 600 | 0, 5, 10, 15, 20, 25, 30, 45, 60, 75, 90, 105, 120, 135, 150 min | 4 |
| Figure 3C | RBP/STRA6 ratio affects the dependence of STRA6 on LRAT | Real-time monitoring of retinol release from holo-RBP | 5X15X10 = 750 | 0, 5, 10, 20, 30, 45, 60, 75, 90, 105, 120, 135, 150, 165, 180 min | 3 |
| Figure 3D | Retinol inhibits STRA6-catalyzed retinol release from holo-RBP | Real-time monitoring of retinol release from holo-RBP | 5X11X10 = 550 | 0, 5, 10, 15, 25, 35, 45, 55, 65, 75, 85 min | 4 |
| Figure 4A | Retinol loading after retinol release and its inhibition by LRAT | Real-time monitoring of retinol release from holo-RBP | 3X18X10 = 540 | 0, 5, 10, 15, 20, 30, 40, 50, 60, 70, 80, 90, 95, 100, 110, 120, 130, 140 min | 3 |
| Figure 4B | STRA6-catalyzed retinol loading into apo-RBP | Real-time monitoring of retinol loading into apo-RBP | 4X17X10 = 680 | 0, 5, 10, 15, 20, 25, 30, 35, 40, 45, 50, 60, 70, 80, 100, 120, 150 min | 6 |
| Figure 4C | STRA6-catalyzed retinol loading as compared to retinol release in 4D | Real-time monitoring of retinol loading into apo-RBP | 3X20X10 = 600 | 0, 2, 5, 10, 15, 20, 25, 30, 35, 40, 45, 50, 55, 60, 70, 80, 90, 100, 110, 120 min | 3 |
| Figure 4D | STRA6-catalyzed retinol release as compared to retinol loading in 4C | Real-time monitoring of retinol release from holo-RBP | 3X20X10 = 600 | 0, 2, 5, 10, 15, 20, 25, 30, 35, 40, 45, 50, 55, 60, 70, 80, 90, 100, 110, 120 min | 3 |
| Figure 4E | Competition between STRA6-catalyzed retinol loading and release | Real-time monitoring of retinol release and retinol loading | 2X14X10 = 280 | 0, 2, 5, 10, 15, 20, 25, 30, 35, 40, 45, 50, 55, 60 min | 5 |
| Figure 4F | Inhibition of STRA6-catalyzed retinol loading by LRAT and CRBP-I | Real-time monitoring of retinol loading into apo-RBP | 3X11X10 = 330 | 0, 2, 5, 10, 15, 20, 25, 30, 40, 50, 60 min | 3 |
| Figure 5A | STRA6-catalyzed transfer of retinol from holo-RBP to EGFP-CRBP-I | Visualization of FRET between retinol and EGFP using fluorometer | 5 | 0, 5, 10, 15, 20 min | 3 |
| Figure 5B | Control FRET experiment in which EGFP is not linked to CRBP-I | Visualization of FRET between retinol and EGFP using fluorometer | 5 | 0, 5, 10, 15, 20 min | 3 |
| Figure 5C | Time course of STRA6-catalyzed retinol transfer to EGFP-CRBP-I | Real-time monitoring of retinol-EGFP FRET | 3X16X10 = 480 | 0, 5, 10, 15, 20, 30, 40, 50, 60, 75, 90, 95, 100, 110, 115, 120 min | 5 |
| Figure 6A | Enhancement of STRA6-catalyzed retinol release by RDH and NADP | Real-time monitoring of retinol release from holo-RBP | 4X18X10 = 720 | 0, 5, 10, 15, 20, 30, 40, 50, 60, 80, 100, 120, 140, 160, 180, 200, 220, 240 min | 3 |
| Figure 6B | STRA6 couples to CRABP-I in retinoic acid uptake by RDH and NADP | Real-time monitoring of retinol release from holo-RBP | 3X5 = 15 | 60 min | 3 |
| Figure 7A | STRA6 couples to CRABP-I in retinoic acid uptake from retinoic acid/RBP | Cellular ³ H-retinoic acid uptake from ³ H-retinoic acid/RBP | 3X6 = 18 | 60 min | 5 |
| Figure 7B | Unlabeled retinol and β-ionone enhance STRA6-mediated ³ H-retinol uptake | Cellular ³ H-retinol uptake from ³ H-retinol/RBP complex | 3X10X10 = 300 | 0, 2, 5, 10, 15, 20, 30, 40, 50, 60 min | 4 |
| Figure 7C | β-ionone stimulates STRA6-catalyzed retinol release from holo-RBP | Real-time monitoring of retinol release from holo-RBP | 3X21X10 = 630 | 0, 2, 5, 10, 15, 20, 30, 40, 50, 60, 61, 65, 70, 80, 90, 91, 95, 100, 110 min | 3 |
| Figure 7D | β-ionone stimulates STRA6-catalyzed retinol release but inhibits retinol loading | Real-time monitoring of retinol release from holo-RBP | 6X8X10 = 480 | 0, 2, 5, 10, 15, 20, 30, 40 min | 3 |
| Figure 7E | Competition between β-ionone and retinol in STRA6-catalyzed retinol release | Real-time monitoring of retinol release from holo-RBP | 4X13X10 = 520 | 0, 2, 5, 8, 10, 12, 15, 20, 25, 30, 35, 40, 45 min | 3 |
| Figure 7E | β-ionone inhibits STRA6-catalyzed retinol loading in a dose-dependent manner | Real-time monitoring of retinol loading into apo-RBP | 8 | 4 hours | 3 |
| Figure 7F | β-ionone enhances STRA6-mediated cellular retinol uptake from human serum | HPLC analysis for cellular retinol uptake from human serum | 6X7 = 42 | 0, 30, 60, 90, 120, 180, 240 min | 3 |
| S. Figure 1A | STRA6 couples to CRBP-I for retinol uptake from holo-RBP but not free retinol | Cellular ³ H-retinol uptake from ³ H-retinol/RBP and free ³ H-retinol | 2 | 4 hours | 3 |
| S. Figure 1B | HPLC analysis of retinol uptake mediated by STRA6 and CRBP-I | HPLC analysis for cellular retinol uptake from holo-RBP | 16X3X3 = 144 | 1, 4, or 6 hours | 3 |
| S. Figure 2 | TTR partially suppresses STRA6-mediated retinol uptake from holo-RBP | Cellular ³ H-retinol uptake from ³ H-retinol/RBP complex | 4X6 = 24 | 60 min | 3 |
| S. Figure 3 | RBP/STRA6 ratio affects the dependence of STRA6 on LRAT in retinol uptake | Cellular ³ H-retinol uptake from ³ H-retinol/RBP complex | 3X4 = 12 | 20 min | 3 |
| S. Figure 4 | STRA6-catalyzed retinol loading into apo-RBP and its inhibition by LRAT | RBP purification and HPLC analysis of retinol loading of RBP | 4 | N/A | 2 |
| S. Figure 5A | Overlap between retinol emission spectrum and EGFP excitation spectrum | Measurement of excitation and emission spectra of retinol and EGFP | 4 | 90 min | 6 |
| S. Figure 5B | Bleaching EGFP leads to increased retinol fluorescence in retinol/EGFP-CRBP-I | Measurement of emission spectra of retinol in retinol/EGFP-CRBP-I | 4 | 90 min | 6 |
| S. Figure 6A | Effect of CRBP-I concentration on STRA6-catalyzed retinol transfer to CRBP-I | Real-time monitoring of retinol-EGFP FRET | 4X18X10 = 720 | 0, 2, 5, 10, 15, 20, 30, 40, 50, 60, 80, 100, 120, 121, 125, 130, 135, 140 min | 3 |
| S. Figure 6B | CRBP-I absorbs retinol from membrane independently from STRA6 | Real-time monitoring of retinol-EGFP FRET | 3X3X13X10 = 1170 | 0, 2, 5, 7, 10, 12, 15, 20, 25, 30, 40, 50, 60 min | 4 |
| S. Figure 6C | CRBP-II is less effective than CRBP-I in competing with BSA in binding retinol | Real-time monitoring of retinol-EGFP FRET | 4X11X10 = 440 | 0, 1, 2, 3, 4, 5, 7, 10, 12, 15, 20 min | 4 |
| S. Figure 6D | Comparison of STRA6-catalyzed retinol transfer to CRBP-I and CRBP-II | Real-time monitoring of retinol-EGFP FRET | 3X11X10 = 330 | 0, 2, 5, 10, 15, 20, 25, 30, 40, 50, 60 min | 3 |

Supplemental References

1. Kawaguchi, R., Yu, J., Honda, J., Hu, J., Whitelegge, J., Ping, P., Wiita, P., Bok, D., and Sun, H. (2007) A membrane receptor for retinol binding protein mediates cellular uptake of vitamin A, *Science* 315, 820-825.
2. Isken, A., Golczak, M., Oberhauser, V., Hunzelmann, S., Driever, W., Imanishi, Y., Palczewski, K., and von Lintig, J. (2008) RBP4 Disrupts Vitamin A Uptake Homeostasis in a STRA6-Deficient Animal Model for Matthew-Wood Syndrome, *Cell Metab* 7, 258-268.
3. Golczak, M., Maeda, A., Bereta, G., Maeda, T., Kiser, P. D., Hunzelmann, S., von Lintig, J., Blaner, W. S., and Palczewski, K. (2008) Metabolic basis of visual cycle inhibition by retinoid and nonretinoid compounds in the vertebrate retina, *J Biol Chem* 283, 9543-9554.
4. Imanishi, Y., Batten, M. L., Piston, D. W., Baehr, W., and Palczewski, K. (2004) Noninvasive two-photon imaging reveals retinyl ester storage structures in the eye, *J Cell Biol* 164, 373-383.
5. Harrison, E. H., and Gad, M. Z. (1989) Hydrolysis of retinyl palmitate by enzymes of rat pancreas and liver. Differentiation of bile salt-dependent and bile salt-independent, neutral retinyl ester hydrolases in rat liver, *J Biol Chem* 264, 17142-17147.
6. Mills, J. P., Furr, H. C., and Tanumihardjo, S. A. (2008) Retinol to retinol-binding protein (RBP) is low in obese adults due to elevated apo-RBP, *Exp Biol Med (Maywood)* 233, 1255-1261.
7. Napoli, J. L. (2000) A gene knockout corroborates the integral function of cellular retinol-binding protein in retinoid metabolism, *Nutr Rev* 58, 230-236.
8. Qtaishat, N. M., Redmond, T. M., and Pepperberg, D. R. (2003) Acute radiolabeling of retinoids in eye tissues of normal and rpe65-deficient mice, *Invest Ophthalmol Vis Sci* 44, 1435-1446.
9. Futterman, S., and Heller, J. (1972) The enhancement of fluorescence and the decreased susceptibility to enzymatic oxidation of retinol complexed with bovine serum albumin, -lactoglobulin, and the retinol-binding protein of human plasma, *J Biol Chem* 247, 5168-5172.
10. Rattner, A., Smallwood, P. M., and Nathans, J. (2000) Identification and characterization of all-trans-retinol dehydrogenase from photoreceptor outer segments, the visual cycle enzyme that reduces all-trans-retinal to all-trans-retinol, *J Biol Chem* 275, 11034-11043.
11. Stryer, L. (1978) Fluorescence energy transfer as a spectroscopic ruler, *Annu Rev Biochem* 47, 819-846.
12. Tsien, R. Y. (1998) The green fluorescent protein, *Annu Rev Biochem* 67, 509-544.
13. Miyawaki, A., Llopis, J., Heim, R., McCaffery, J. M., Adams, J. A., Ikura, M., and Tsien, R. Y. (1997) Fluorescent indicators for Ca²⁺ based on green fluorescent proteins and calmodulin, *Nature* 388, 882-887.
14. Imanishi, Y., Gerke, V., and Palczewski, K. (2004) Retinosomes: new insights into intracellular managing of hydrophobic substances in lipid bodies, *J Cell Biol* 166, 447-453.
15. Zanotti, G., and Berni, R. (2004) Plasma retinol-binding protein: structure and interactions with retinol, retinoids, and transthyretin, *Vitam Horm* 69, 271-295.